

## **Layer-dependent Anisotropic Frictional Behavior in Two-dimensional Monolayer Hybrid Perovskite/ITO Layered Heterojunctions (supporting)**

Sheng Bi<sup>1,2</sup>; Qikun Li<sup>2</sup>; Ying Yan<sup>1</sup>; Kyeiwaa Asare-Yeboah<sup>3</sup>; Tianbao Ma<sup>4</sup>; Chaolong Tang<sup>5</sup>; Zhongliang Ouyang<sup>6</sup>; Zhengran He<sup>6</sup>; Yun Liu<sup>7</sup>; Chengming Jiang<sup>1,2,\*</sup>

1 Key Laboratory for Precision and Non-traditional Machining Technology of the Ministry of Education, Dalian University of Technology, Dalian 116024, China

2 Institute of Photoelectric Nanoscience and Nanotechnology, School of Mechanical Engineering, Dalian University of Technology, Dalian 116024, China

3 Department of Electrical and Computer Engineering, Penn State Behrend, Erie, PA 16563, USA

4 State Key Laboratory of Tribology, Tsinghua University, Beijing 100084, China

5 School of Physical & Mathematical Science, Nanyang Technological University, 637371, Singapore

6 Department of Electrical and Computer Engineering, Center for Materials for Information Technology, The University of Alabama, Tuscaloosa, AL, 35487, USA

7 School of Physics, Dalian University of Technology, Dalian 116024, China

\*E-mail: [jiangcm@dlut.edu.cn](mailto:jiangcm@dlut.edu.cn)

## 1, AFM lateral force calibration:

The dimensions of the cantilever, containing length, mean width ( $l$ ), thickness ( $t$ ) and tip height ( $h$ ) are confirmed by SEM (scanning electron microscope) firstly.

Then the lateral spring constant  $k_l$  can be obtained from<sup>[3]</sup>

$$k_l = \frac{Gwt^3}{3l(h + t/2)^2} \quad (\text{S1})$$

where  $G$  is the cantilever shear modulus.

The lateral sensitivity of AFM, which is inherent attribute of cantilever system, is defined as the ratio between the photodiode voltage and the deflection of the AFM cantilever

$$S_l = \frac{V_l}{x_l} \quad (\text{S2})$$

where  $v_l$  is the corresponding photodiode voltage outputs and  $x_l$  is the deformation in lateral direction. In the cross-section view of the cantilever which is rectangular shape, the lateral force  $F_l$  is derived from the measured photodiode voltage  $V_l$ ,

$$F_l = \frac{k_l}{S_l} V_l = \alpha_l V_l \quad (\text{S3})$$

where  $\alpha$  is defined as the transition coefficient.

Actually,  $\alpha$  is also calibrated by the projection plane as the figure shown below.<sup>[4,5]</sup>

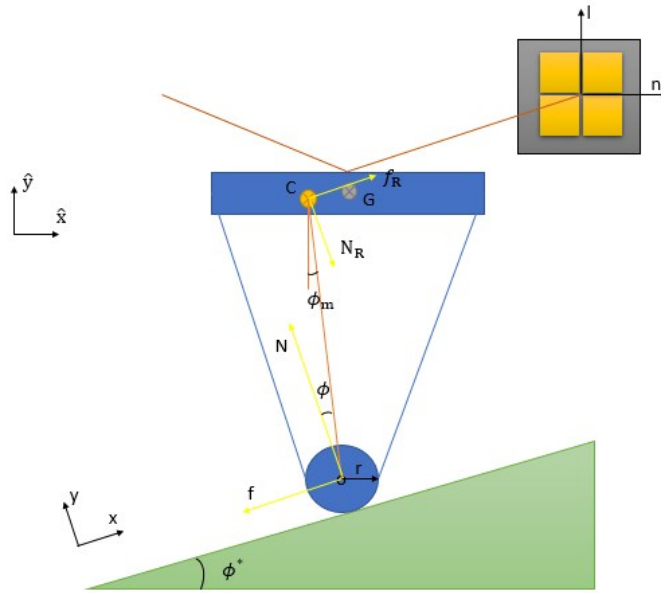


**Figure S1.** The cross-section schematic of the tip contacted with the surface of a typical material.

Figure S1 is the front view diagram of an AFM cantilever of the deformed configuration on a projection plane. In this section, the mechanical interference effect and the optical misalignment effect will be taken into consideration.

Firstly, it is assumed that the tip is locally spherical with radius  $r$  and the center point at  $O$ , as presented in the figure. It is assumed that the normal force  $F$  is perpendicular to the projection plane. The shear deformation center of the AFM cantilever  $C$  is an inherent point of structural feature, which depends on the distribution of the elastic modulus and the entire geometry of the whole cantilever. In general, the point  $C$  is distinctly misalign with the geometrical center  $G$  of cantilever. The length  $h$  of  $OC$

is the arm of force of  $f$ . The angle  $\phi = \phi_i + \delta\phi$ , in which  $\phi_i$  is the initial tilt angle in the undeformed configuration and  $\delta\phi$  is the twist angle with little deformation. It is obvious that the force balance  $f_R = f$  which denotes the lateral force and  $N_R = N$  which denotes the normal force at the contact point. The moment balance with the asymmetry contact moment under the shear deformation center C can be expressed as

$$M = Nh \sin \phi + f(h \cos \phi + r) - M_m \quad (\text{S4})$$

The torsional moment  $M$  is a elastic torsional deformation and can be expressed as

$$M = \eta \delta\phi \quad (\text{S5})$$

where  $\eta$  is the torsional spring constant of AFM cantilever.

$\delta\phi$  is the small deformation, and it always follows the equation below

$$Nh \sin \phi_i + f(h \cos \phi_i + r) - M_m = \eta^* \delta\phi \quad (\text{S6})$$

where the effect constant is  $\eta^* = (\eta - Nh \cos \phi_i + fh \sin \phi_i) \cong \eta^*$  for  $\frac{Nh}{\eta} \ll 1$  and

$\frac{fh}{\eta} \ll 1$  in typical AFM.

As equation expressed in eq.(S2), AFM output voltage  $V$  in lateral direction with twisted angle  $\delta\phi$  can be express as

$$V_l = S_l^a \delta\phi \quad (S7)$$

where  $S_l^a$  is the lateral angle sensitivity. The  $S_l^a$  which is expressed as  $S_l^a = \eta / s$  is related to the calibration parameters.  $\phi_i$  in Eq.(S6) can be replaced by  $\phi_i = \phi^* - \phi_m$ .

$$N_{\pm} (1 - \gamma) \sin(\phi^* - \phi_m) \pm f_{\pm} [(1 - \gamma) \cos(\phi^* - \phi_m) + \gamma] = \alpha_l V_{l\pm} \quad (S8)$$

where  $\pm$  denotes  $f_R$  in  $\hat{x}$  forward and backward directions, respectively,  $\alpha_l$  is generic lateral force constant as shown in eq.(S3), and  $V$  equals to  $r/(h+r)$ .

In the situation of  $M/f(h+r) \ll 1$ , the  $\alpha_l$  is defined as

$$\alpha_l = \frac{\eta}{S_l(h+r)} \quad (S9)$$

The  $\alpha_l$  can be directly calibrated by regulating the variation of  $V_l$  to make  $N$  vanish when the substrate angle is to be  $\phi_i = 0$ . The lateral force can be expressed as

$$f_{\pm} = \pm \alpha_l V_{l\pm} \quad (S10)$$

In most cases, AFM thin film cantilever is parallel to the scanning plane, and the conversion array can be defined as

$$\begin{pmatrix} N_{\pm} \\ f_{\pm} \end{pmatrix} = \begin{pmatrix} \cos \phi^* & \pm \sin \phi^* \\ \mp \sin \phi^* & \cos \phi^* \end{pmatrix} \begin{pmatrix} \hat{N}_{\pm} \\ \hat{f}_{\pm} \end{pmatrix}$$

The interference constant  $\alpha_{nl}$  is negligible because the lateral force in normal direction has little impact on the cantilever. Therefore, three force constants,  $\alpha_n$ ,  $\alpha_{ll}$ ,  $\alpha_{ln}$ , are calibrated, where  $\alpha_n$  is the constant in the normal direction,  $\alpha_{ll}$  is in lateral direction and  $\alpha_{ln}$  is the interference constant in lateral direction. The lateral force and normal force can be presented as

$$f_{\pm} = \pm (\alpha_{ll}V_l + \alpha_{ln}V_n)$$

$N_{\pm} = \pm \alpha_n V_{n\pm}$  where  $V_n$  and  $V_l$  are the output voltage of normal and lateral deformation. The  $\alpha_{ln}$  and  $\alpha_{ll}$  can be derived from

$$\alpha_{ll} = \alpha_l [(1 - \gamma)\cos \phi_m + \gamma\cos \phi^*]$$

$$\alpha_{ln} = \alpha_n \frac{(1 - \gamma)\sin \phi_m + \gamma\sin \phi^*}{(1 - \gamma)\cos \phi_m + \gamma\cos \phi^*}$$

It is noticed that  $\alpha_{ll}$ ,  $\alpha_{ln}$  equals to  $\alpha_l$  when  $\phi_m$  and  $\phi^*$  equal to 0. When  $\phi^*$  equals to 0,  $\alpha_{ln}$  is negligible and the  $\alpha_{ll}$  is expressed as

$$\alpha_{ll} = \frac{\eta}{S_l(h + r)[(1 - \gamma)\cos \phi_m + \gamma]}$$

## 2, Other details

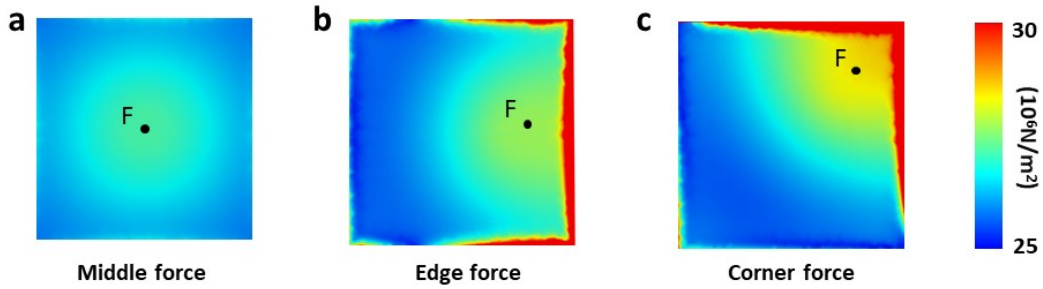


Figure S2. The simulation results of the force distribution on  $2\mu\text{m}$  by  $2\mu\text{m}$   $\text{SiO}_2$  cap with  $10\mu\text{N}$  applied force at different applied position.

The force distribution on the sample at different positions is simulated by Finite Element Analysis, as shown in Figure S2. From the results, it is clearly seen that, when the AFM tip is applied at the middle of the square, the force difference at different positions is the smallest, comparing with the other situations. At the same time, the  $\text{SiO}_2$  has a high Young's modulus of  $6.6 \times 10^{10} \text{ N/m}^2$ . In this experiment, little deformation occurred on the cap, which can be treated as an ideal rigid body. Therefore, while the AFM tip is applied at the middle of the square, the force can be treated as a uniformly distributed force on the sample.

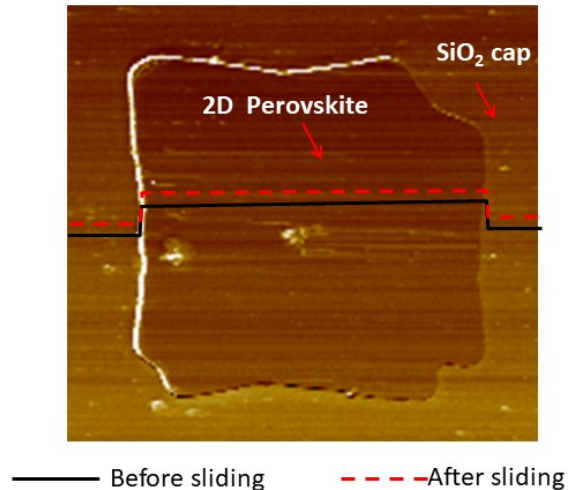


Figure S3. The topography scanned by AFM of the 2D perovskite on the SiO<sub>2</sub> cap. The solid black line and the dash red line are the moving paths across the 2D perovskite sheet before and after sliding using AFM tip under non-contact mode position scanning lines on the same sample. It proves that the 2D perovskite sheet remains at the same position on SiO<sub>2</sub> cap before and after sliding.

We use AFM non-contact mode to scan the topography of the sample before and after sliding, as shown in Figure 2. By comparison of the two results, it is clearly shown that the perovskite sheet has no displacement on the SiO<sub>2</sub> cap from its original position. Therefore, the contact between perovskite sheet and SiO<sub>2</sub> is strong enough to prove the correctness of the result.

Reference:

- [1] L. Dou, A. B. Wong, Y. Yu, M. Lai, N. Kornienko, S. W. Eaton, A. Fu, C. G. Bischak, J. Ma, T. Ding, N. S. Ginsberg, L. W. Wang, A. P. Alivisatos, P. Yang, *Science* (80-. ). **2015**, *349*, 1518.
- [2] Z. Tan, Y. Wu, H. Hong, J. Yin, J. Zhang, L. Lin, M. Wang, X. Sun, L. Sun, Y. Huang, K. Liu, Z. Liu, H. Peng, *J. Am. Chem. Soc.* **2016**, *138*, 16612.
- [3] H. Xie, J. Vitard, S. Haliyo, S. Régnier, M. Boukallel, *Rev. Sci. Instrum.* **2008**, *79*, 033708.
- [4] Q. Li, K.-S. Kim, A. Rydberg, *Rev. Sci. Instrum.* **2006**, *77*, 065105.
- [5] H. Wang, *Sci. Adv. Mater.* **2017**, *9*, 56.